

Elastic–Plastic Spherical Contact Modeling Including Roughness Effects

L. Li · I. Etsion · F. E. Talke

Received: 29 June 2010 / Accepted: 14 October 2010 / Published online: 28 October 2010
© The Author(s) 2010. This article is published with open access at Springerlink.com

Abstract The effect of material properties and surface roughness on the contribution of asperities and sphere bulk displacements to the total displacement of a rough spherical contact is investigated. A dimensionless transition load, above which the contribution of the bulk displacement exceeds the contribution of the asperities displacement, is found as a function of the plasticity index and dimensionless critical interference of the sphere bulk. A criterion is proposed for evaluating the importance of surface roughness in calculating the displacement of a rough spherical contact. Some experimental results with a spherical micro-contact are presented to verify the model.

Keywords Contact mechanics · Spherical contact · Rough surface · Plasticity index

List of symbols

a_n Nominal radius of contact
 C_v $1.234 + 1.256v$
 d Separation based on asperity heights
 d^* Dimensionless separation, d/σ
 E Young's modulus
 h_0 Minimum separation
 h_0^* Dimensionless minimum separation, h_0/σ
 h_1 Displacement of the contacting asperities

h_1^* Dimensionless displacement of the contacting asperities, h_1/σ
 L_c Critical normal load in full stick
 P Normal load
 P_c Critical normal load in perfect slip, $\frac{\pi^3}{6} C_v^3 Y (R(1-v^2) \frac{Y}{E})^2$
 P^* Dimensionless normal load, for stick P/L_c and for slip P/P_c
 R Radius of the sphere
 r Radial coordinate
 r^* Dimensionless radial coordinate, $r/\sqrt{R\sigma}$
 Y Yield strength
 z Asperity height
 z^* Dimensionless height, z/σ
 β Roughness parameter, $\eta\rho\sigma$
 γ Total displacement of the rough spherical contact
 γ^* Dimensionless total displacement, γ/σ
 δ_c Critical interference of an asperity in full stick, $\bar{\delta}_c\omega_c$
 $\bar{\delta}_c$ $6.82v - 7.83(v^2 + 0.0586)$
 δ_c^* Dimensionless critical interference, δ_c/σ
 η Area density of asperities
 ρ Asperity tip radius of curvature
 σ Standard deviation of surface heights
 σ_s Standard deviation of asperity heights
 ν Poisson's ratio
 ψ Plasticity index, $\frac{2E}{C_v\pi(1-\nu^2)Y} \left(\frac{\sigma_s}{\rho}\right)^{0.5}$
 ω Displacement of the sphere bulk
 ω^* Dimensionless displacement, ω/σ
 ω_c Critical interference of the sphere bulk, $\left(\frac{C_v\pi(1-\nu^2)Y}{2E}\right)^2 R$
 ω_c^* Dimensionless critical interference of the sphere bulk, ω_c/σ

L. Li
Harbin Institute of Technology, Harbin 150001, China

L. Li · F. E. Talke
University of California, San Diego, La Jolla,
CA 92093-0401, USA

I. Etsion (✉)
Technion-Israel Institute of Technology, Haifa 32000, Israel
e-mail: etsion@technion.ac.il

1 Introduction

The evolution of the contact of rough surfaces is an important problem in contact mechanics [1] and tribology. Contact starts at the summits of the highest asperities, i.e., the real contact area is likely to be only a small fraction of the nominal contact area. The number of contacting asperities, as well as the real contact area, increases with increasing normal load. Greenwood and Williamson (GW) presented a theoretical model for contact of nominally flat rough surfaces [2]. They assumed that displacement occurs only at the contacting asperities, i.e., bulk displacement is absent. In addition, they assumed that the asperities displacement is purely elastic. Greenwood and Williamson also recognized that with increasing roughness, asperities plastic deformation may occur. To take account of this case, they introduced a dimensionless parameter, the plasticity index ψ , to determine the conditions for which their elastic model becomes invalid.

Different from nominally flat surfaces, in a rough spherical contact, both the contacting asperities and the bulk material of the sphere deform under normal load. Hence, the total displacement includes contributions of both the asperities and bulk material. Several studies dealing with contact of rough spherical surfaces can be found in the literature. Greenwood and Tripp [3] presented a model for the elastic contact of rough spheres. Using an iterative solution, they calculated the displacement of both the asperities and the sphere. They found that for light loads the total displacement at the center of the contact area is mainly due to the displacement of asperities, for high loads the total displacement is mainly due to bulk displacement of the sphere. Kagami et al. [4] analyzed the contact of a smooth sphere loaded against a rough flat. They presented a “mixed asperity contact” model, in which they assumed elastic or plastic deformation of asperities below or above a critical deformation, respectively. Experimental results for the contact radii and the total displacement are also presented in [4] as a function of normal load for rough and smooth copper and steel plates indented by a smooth steel sphere. They found that a rough spherical contact at low normal loads produces a lower contact pressure distribution and a larger contact radius compared to the Hertz solution for a smooth spherical contact. At high normal loads the roughness effect diminishes.

Greenwood et al. [5] examined the influence of surface roughness and investigated the contact pressure and contact area between a sphere and a plane. They proposed that the influence of surface roughness is governed by a single dimensionless parameter α defined by

$$\alpha = \frac{\sigma R}{a^2}, \quad (1)$$

where σ is the combined roughness of the two contacting surfaces, R is the radius of the sphere, and a is the contact radius for contact of smooth surfaces given by the Hertz theory. It should be noted that in purely elastic contact the parameter α is in fact the ratio σ/ω , where ω is the displacement of the smooth sphere. According to Greenwood et al. [5], the effect of roughness is negligible if α is < 0.05 .

Bahrami et al. [6] presented a model in which an elastic half space covered by plastically deformed asperities is indented by a rigid sphere. They observed good correlation between their theoretical results and the experimental results of Refs. [4] and [5] for the contact radius and compliance. Wang et al. [7] presented a multilevel contact model for a rough spherical contact and investigated the surface roughness effect on the real contact area. In their model, the total deformation was composed of the displacement of the bulk and asperities. Jamari and Schipper [8] evaluated the displacement behavior of the contact between a real rough flat surface and a smooth ball. They allowed three displacement responses: plastic deformation of the asperities only, plastic deformation of the bulk only, and combined plastic deformation of both the asperities and the bulk. They measured the contact area of aluminum and brass flats that were indented by a harder steel sphere and found good agreement between experimental results and theoretical predictions.

In Refs. [3–7], the total compliance of the rough spherical contact is provided without separating the individual contributions of bulk and asperities. Only in Ref. [8] such separation is made but as in Refs. [3–7] the bulk deformation of the sphere is assumed to be purely elastic. Furthermore, the displacement of the asperities in Refs. [3–8] is assumed to be purely elastic and/or ideal plastic.

Recently, Cohen et al. [9] and Li et al. [10] analyzed the contact of a rough sphere loaded by a rigid flat and relaxed previous simplifying assumptions regarding bulk and asperity deformation. They assumed that the sphere and the asperities on the sphere can have any combination of elastic, elastic–plastic, and fully plastic deformation. The main goal in those two papers was the prediction of real contact area and static friction and hence, only flattening of the asperities was reported.

The main goals of the present work are (a) to investigate the contact between a rough sphere and a rigid flat and determine the individual contributions of the asperities and the bulk of the sphere to the total displacement and (b) to find a dimensionless parameter similar to α in Eq. 1 that will not be limited to elastic displacement only.

2 Theoretical Analysis

As indicated in [3], the total displacement of a rough spherical contact is composed of displacements of both the asperities and the bulk of the sphere. Hence, the total displacement γ can be defined as

$$\gamma = \omega + h_1, \tag{2}$$

where ω and h_1 are the displacement of the sphere bulk and the asperities on the sphere, respectively.

A model of the rough spherical contact is presented in Fig. 1. As shown in Refs. [9] and [10], the roughness of the sphere can be transferred to the flat without affecting the original contact problem. The contacting asperities and the sphere deform to provide a real contact area that supports the normal load P . The deformation of the asperities and the sphere can be elastic, elastic–plastic, fully plastic or any combination of the three types of deformation. The peak of the sphere is flattened, due to its displacement ω , forming a circular contact area with radius a_n over which a uniform separation h_0 is assumed between the sphere and the mean of the surface heights of the rough flat. It should be noted here that representing the rough circular contact area as a flat is only a simplified approximation. The entire nominal contact area, in the presence of roughness, may be curved and its total size may be larger than the flat portion shown in Fig. 1. This larger size is accounted for in the present model by considering also asperity contact with the curved surface of the sphere outside the flattened area of radius a_n . In the following, parameters that have dimensions of length in the radial direction are normalized by $\sqrt{R\sigma}$, parameters with dimensions of length in the normal direction are normalized by σ and are denoted with * [9].

As shown in Ref. [9], the separation h^* outside the flattened region has the form

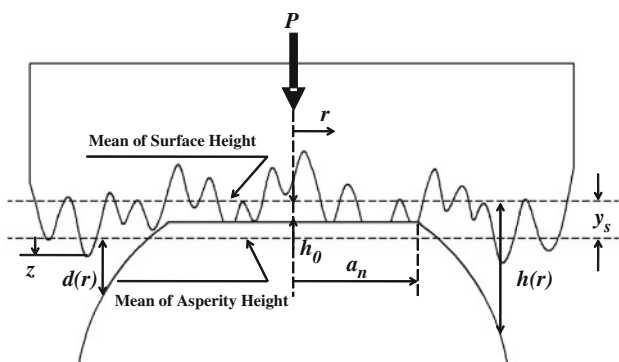


Fig. 1 Contact model for a rough sphere and a rigid flat showing an equivalent rough flat and a smooth sphere

$$h^*(r^*) = \begin{cases} \frac{1}{\pi\psi^2\rho/R}P^{*2/3}f^*(r^*) + h_0^* & 0 \leq P^* \leq 1 \\ \frac{0.951}{\pi\psi^2\rho/R}\left(\frac{P^*}{1.03}\right)^{0.809}f^*(r^*) + h_0^* & 1 \leq P^* \leq 13.3 \\ \frac{0.457}{\pi\psi^2\rho/R}\left(\frac{P^*}{1.40}\right)^{1.249}f^*(r^*) + h_0^* & 13.3 \leq P^* \leq 530 \end{cases}, \tag{3}$$

where ρ is the asperity summit radius and $f^*(r^*)$ is given by (see [10])

$$f^*(r^*) = a_n^*\sqrt{r^{*2} - a_n^{*2}} - (2a_n^{*2} - r^{*2}) \tan^{-1}\left(\frac{r^{*2}}{a_n^{*2}} - 1\right)^{1/2} \tag{4}$$

The dimensionless normal load P^* between the two contacting surfaces under full stick contact condition is obtained from [10] as

$$P^* = \frac{P}{L_c} = \frac{2\pi\beta\psi^3\rho}{(\bar{\delta}_c)^{1.5}R} \int_0^{R^*} r^* \left[\int_{h^*-y_s^*}^{h^*-y_s^*+\delta_c^*} (z^* - h^* - y_s^*)^{3/2} \phi^*(z^*) dz^* + \int_{h^*-y_s^*+\delta_c^*}^{h^*-y_s^*+110\delta_c^*} (z^* - h^* - y_s^*)^{3/2} (1 - I^\alpha) \phi^*(z^*) dz^* + 4.6 \frac{\bar{\delta}_c^{1/2}}{\psi} \int_{h^*-y_s^*+110\delta_c^*}^\infty (z^* - h^* - y_s^*) \phi^*(z^*) dz^* \right] dr^*, \tag{5}$$

where the integrand I^α is given by (see [9])

$$I^\alpha = \exp \left[\left(1 - \left((z^* - h^* - y_s^*) \frac{\psi^2(\sigma/\sigma_s)}{\bar{\delta}_c} \right)^\alpha \right)^{-1} \right] \tag{6}$$

In Eqs. 5 and 6, $\bar{\delta}_c$ is the ratio δ_c/ω_c of the critical interference in full stick over that in perfect slip [11], ϕ^* is the distribution function of asperity heights, and y_s is the distance between the mean of the asperity heights and the mean of the surface heights (see Fig. 1). In this work, a Gaussian distribution is used. Additional details can be found in Ref. [10].

When the dimensionless separation $h_0^* > 3$ the number of asperities in contact is very small [12] and the surfaces are nearly separated. Hence, assuming that contact begins at $h_0^* = 3$ when both the normal load and the displacement of the asperities are zero, one can obtain the displacement of the asperities in the form

$$h_1^* = 3 - h_0^* \tag{7}$$

The dimensionless displacement of the bulk of the sphere under slip contact condition is given by the following expression (see Ref. [13])

$$\frac{\omega}{\omega_c} = \begin{cases} P^{*2/3}, & 0 \leq P^* \leq 1 \\ \left(\frac{P^*}{1.03}\right)^{0.702}, & 1 \leq P^* \leq 13.3 \\ \left(\frac{P^*}{1.40}\right)^{0.801}, & 13.3 \leq P^* \leq 530 \end{cases} \quad (8)$$

where ω_c is the critical interference of the bulk of the sphere at yield inception under slip contact condition and P^* is the load P normalized by P_c . It should be noted that for $\nu > 0.25$ the critical interference and critical load in slip and in stick contact condition are almost the same [11]. Hence, in the following we shall replace L_c by P_c to express P^* .

Using Eq. 8, one can express the dimensionless displacement of the bulk of the sphere ω/σ in the form

$$\omega^* = \frac{\omega}{\omega_c} \quad \omega_c^* = \begin{cases} \omega_c^* P^{*2/3}, & 0 \leq P^* \leq 1 \\ \omega_c^* \left(\frac{P^*}{1.03}\right)^{0.702}, & 1 \leq P^* \leq 13.3 \\ \omega_c^* \left(\frac{P^*}{1.40}\right)^{0.801}, & 13.3 \leq P^* \leq 530 \end{cases} \quad (9)$$

The total dimensionless displacement $\gamma^* = \gamma/\sigma$ is the sum of the individual contributions of the asperities and the bulk displacements (see Eq. 2) and hence, it depends on the dimensionless normal load P^* , the plasticity index ψ , and the parameter ω_c^* .

$$\gamma^* = \omega^* + h_1^* \quad (10)$$

3 Results and Discussion

In this investigation, we use the same values of Poisson's ratio ($\nu = 0.3$) and surface roughness parameter ($\beta = 0.04$) as used in Refs. [9, 10]. An iterative solution (see Ref. [9]) was implemented to obtain the dimensionless normal load P^* for varying separation h_0^* (and, hence, h_1^* , see Eq. 7) as a function of the plasticity index ψ . Then, ω^* was obtained from Eq. 9 for the calculated P^* values at various values of ω_c^* . Note that for $\sigma \approx \sigma_s$ it is reasonable to express ω_c^* in the form (see List of symbols):

$$\omega_c^* = \frac{R}{\rho} \psi^{-2} \quad (11)$$

This approximation may be valid even when σ is up to 10% smaller than σ_s since the error in ψ (see List of symbols), which is related to the square root of the error in σ_s , will be no more than 5%. Substituting the ratio ρ/R from Eq. 11 in Eqs. 3 and 5, we observe that Eq. 5 is independent of ρ/R . Hence, the parameters for the problem at hand are ψ and ω_c^* . Furthermore, as will be seen later, the results obtained from Eq. 5 are independent of ω_c^* . Hence, ψ affects the displacement of the asperities and ω_c^* affects the displacement of the sphere bulk.

Figure 2 shows the effect of the critical interference ω_c^* on the relation between the dimensionless normal load P^* and the individual displacements h_1^* and ω^* of the

asperities and the bulk of the sphere, respectively, along with their sum (the total displacement) γ^* . The results are presented for a typical plasticity index $\psi = 2$ and three different values of $\omega_c^* = 1, 2,$ and 5 . The combination of the displacement of the bulk of the sphere and asperities can be described as a system of two nonlinear springs in series (see, e.g., [14]). Initially, at small loads, the stiffness of the asperities is much smaller than that of the bulk and hence, the contribution of the asperities to the total displacement is dominant. As the load P^* increases the asperities are flattened, their stiffness increases rapidly and becomes larger than that of the bulk. Eventually, at a dimensionless transition load P_t^* the bulk displacement equals the displacement of the asperities. At $P^* > P_t^*$ the additional displacement of the stiffer asperities contributes very little to the increase of the total displacement and the bulk contribution becomes the dominant one. For $\omega_c^* = 1$, shown in Fig. 2a, the transition load is about $P_t^* = 16$. As ω_c^* increases (see Fig. 2b, c) the dimensionless transition load P_t^* decreases. Rearranging Eq. 9 to express P^* as a function of ω^* it can be seen that the dimensionless stiffness of the bulk $\partial P^*/\partial \omega^*$ decreases with increasing ω_c^* . A lower dimensionless stiffness of the bulk material increases the displacement at a given load and hence, reduces the dimensionless transition load P_t^* with increasing ω_c^* .

In Figs. 2a and 3, the effect of the plasticity index ψ on the relation between the normal load P^* and the displacement components is presented. The results are shown for a typical dimensionless critical interference $\omega_c^* = 1$ and three values of the plasticity index $\psi = 2, 5,$ and 8 . As can be seen from these figures, as ψ increases, a higher load P^* is required for a given displacement h_1^* of the asperities. This is due to increased dimensionless stiffness of the asperities with increasing ψ [12]. Increased stiffness of the asperities affects the transition load in the same way as decreased stiffness of the bulk. Therefore, the dimensionless transition load P_t^* decreases with increasing ψ .

Figure 4 shows the combined effect of the controlling parameters ω_c^* and ψ on the dimensionless transition load P_t^* . As observed from the figure, for small values of both ω_c^* and ψ , the transition load P_t^* is very large, i.e., the contribution of the asperities to the total displacement is dominant. On the other hand, large ω_c^* or large ψ reduces P_t^* to very small values and hence, the contribution of the bulk to the total displacement becomes dominant. The results shown in Fig. 4 were curve fitted yielding the following empirical expression (with R^2 value above 0.99)

$$P_t^* = \left(75.8(\omega_c^*)^{-1.7} + 4.7\right) \psi^{0.01\omega_c^* - 0.16} - \left(51.3(\omega_c^*)^{-1.7} + 4.7\right) \quad (12)$$

The dimensionless parameter P_t^* can be looked upon as a criterion for the importance of the effect of roughness on

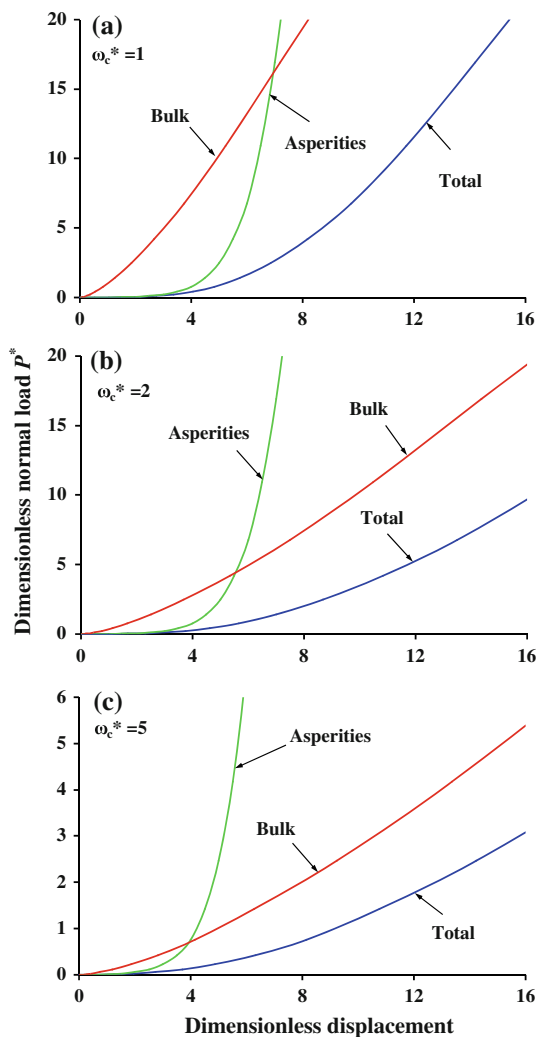


Fig. 2 Dimensionless normal load P^* versus dimensionless displacement of asperities h_1^* , sphere bulk ω^* , and the total displacement γ^* for $\psi = 2$ and dimensionless critical interference: **a** $\omega_c^* = 1$, **b** $\omega_c^* = 2$, and **c** $\omega_c^* = 5$

the total displacement of a rough spherical contact. If $P^* < P_t^*$, the effect of the roughness on the total displacement must be considered. On the other hand, if P^* is much larger than P_t^* , the contribution of the asperities can be neglected. A similar roughness effect on static friction coefficient and junction growth of a rough spherical contact was recently observed experimentally by Ovcharenko et al. [15, 16], and predicted theoretically by Cohen et al. [9]. In all these studies, the effect of surface roughness was found to diminish with an increase in the normal load above a threshold value. Interestingly, a somewhat similar transition load was observed in a nano-spherical contact [17] where the effect of an adsorbed layer on junction growth is investigated. Apparently, the effect of splaying out of adsorbed layers is similar to that of flattening asperities.

It may be argued that some of the assumptions made in this study are oversimplification of an actual rough

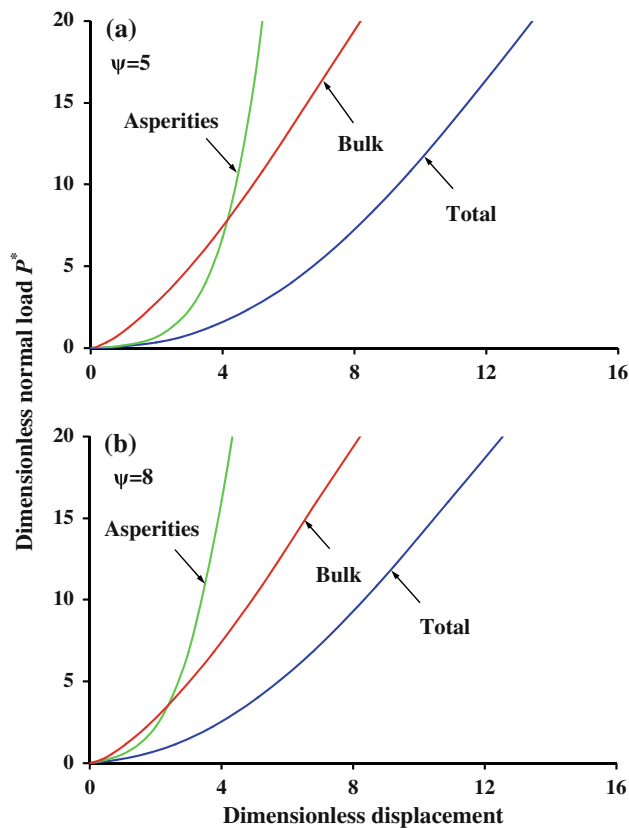


Fig. 3 Dimensionless normal load P^* versus dimensionless displacement for asperities h_1^* , sphere bulk ω^* , and the total displacement γ^* for $\omega_c^* = 2$ and plasticity index: **a** $\psi = 5$ and **b** $\psi = 8$

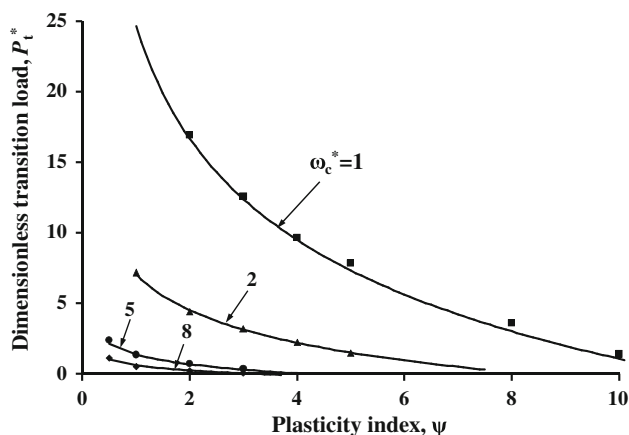


Fig. 4 Dimensionless transition load P_t^* as functions of the plasticity index ψ and ω_c^*

spherical contact. For example, a central flat contact area (see Fig. 1), which is typical for a smooth spherical contact, may not be adequate in the presence of roughness. Also, assuming Gaussian distribution of asperity heights requires an adequate statistical sample of asperity contacts. This can be reasonably met for many contact problems of nominally flat surfaces but may be questionable in

concentrated contact problems, especially under low load with corresponding small contact area typical of elastic spherical contact (see Ref. [3]). A discussion of the real area of contact and real contact pressure is provided in Ref. [3]. It reveals that the variation of the mean real pressure with load in elastic rough spheres is very similar to that in elastic rough flat surfaces. This finding supports the present assumption of central flat contact area.

Another issue is that contact at nano-micro scales can be influenced by effects specific for these scales including effects of size-dependent plasticity (see, e.g., Ref. [18]), local anisotropy of contacting asperities and adhesion. The best way to clarify such issues and test the validity of the model is through experimental verification, as described in the following section.

4 Comparison with Experimental Results

Some preliminary experiments were performed in order to test the validity of the proposed contact model. A stainless steel (SST304) spherical specimen with a radius of $R = 200 \mu\text{m}$ (see Fig. 5) was loaded against a rigid smooth sapphire flat using a modified nano-indenter test rig (Hysitron, Inc., USA). The spherical specimen has a yield strength $Y = 1.68 \text{ GPa}$, Young's modulus $E = 181 \text{ GPa}$, and Poisson's ratio $\nu = 0.31$. With these material properties, the critical interference and critical load of the sphere are (see List of symbols) $\omega_c = 186 \text{ nm}$ and $P_c = 212 \text{ mN}$, respectively. The surface roughness of the spherical specimen was measured by an atomic force microscope (AFM, Pacific Nanotechnology, USA) using a scan size of $10 \times 10 \mu\text{m}^2$ and a sampling interval of $0.69 \mu\text{m}$. The

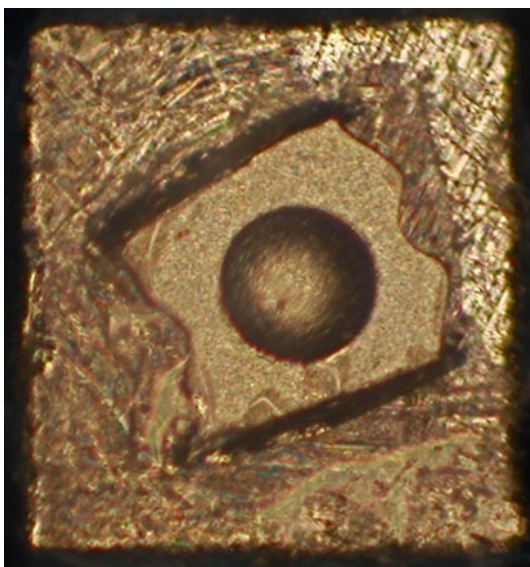


Fig. 5 Top view of the spherical specimen

roughness parameters, calculated from these measurements, were $\rho = 8.30 \mu\text{m}$ and $\sigma \approx \sigma_s = 90 \text{ nm}$. The sapphire flat has a negligible roughness σ of only 4 nm , $Y = 2.95 \text{ GPa}$, Young's modulus $E = 435 \text{ GPa}$, and Poisson's ratio $\nu = 0.27$. Using the above material properties and roughness parameters the resulting value of the plasticity index is $\psi = 3$, the dimensionless critical interference is $\omega_c^* = 2$, and the dimensionless transition load (see Eq. 12) is $P_t^* = 3.03$, which for $P_c = 212 \text{ mN}$ corresponds to a dimensional value of $P_t = 642 \text{ mN}$. The loading range of the nano-indenter is no more than 10 mN , much below the transition load. Hence, according to the model prediction, a dominant contribution of the asperities to the total displacement should be expected.

Figure 6 shows a comparison between the measured total displacement versus normal load (solid line) and the theoretical prediction (dashed lines). As can be seen from the figure, the theoretical total displacement, predicted by the contact model, correlates well with the experimental results. Also, the contribution of the asperities to the total displacement is dominant as predicted by the model for loads much below the transition load.

Finally, Fig. 7 shows an AFM image of the rough sphere after unloading from a 9 mN normal load corresponding to $P^* = 0.04$. A certain portion of the contact area zone is shown encircled. It clearly demonstrates the substantial flattening of contacting asperities compared to all the other original asperities, which were outside the contact area. The very small normal load of 9 mN ($P^* = 0.04$) caused very small elastic deformation of the sphere bulk but the asperities have large plastic deformation. It can also be seen from the figure that there was an adequate statistical sample of asperity contacts to justify the assumption of Gaussian distribution of asperity heights. Hence, these preliminary experimental results verify the contact model and justify its simplifying assumptions.

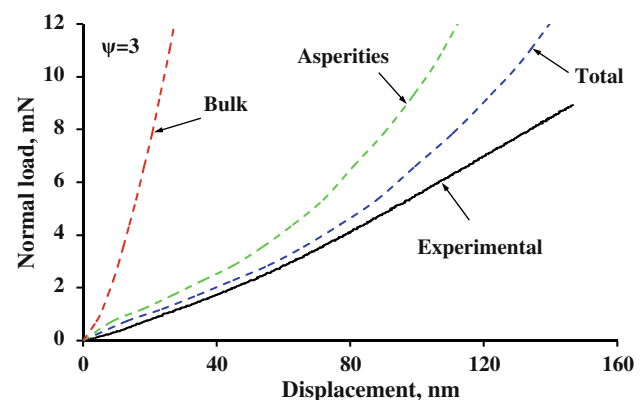


Fig. 6 Comparison of experimental results (solid line) and theoretical predictions (dashed lines) for normal load versus displacement of a rough spherical sample having $\psi = 3$ and $\omega_c^* = 2$

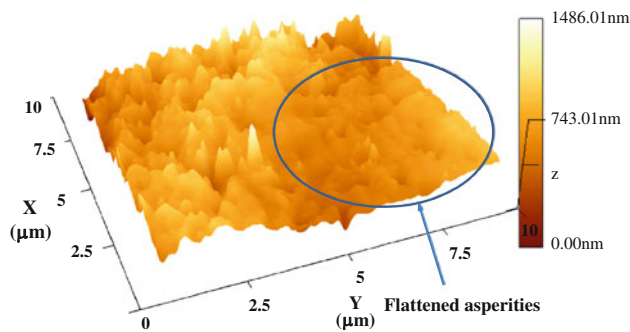


Fig. 7 AFM image of surface roughness of a rough sphere after 200 load-unload cycles, showing the flattened asperities within the encircled portion of the contact area

5 Conclusion

The effect of critical interference and plasticity index on the contributions of asperities and sphere bulk to the total displacement of a rough spherical contact was investigated. A dimensionless transition load P_t^* was found as a function of the bulk critical interference ω_c^* and the plasticity index ψ . This transition load decreases with an increase in ω_c^* and ψ . At loads much smaller than the dimensionless transition load the stiffness of the asperities is smaller than that of the bulk of the sphere and the asperity displacement is dominant. At loads above the transition load the contribution of the bulk to the total displacement becomes larger than the contribution of the asperities. At loads much larger than the dimensionless transition load, the roughness effect is negligible. Preliminary experimental results verified the theoretical predictions and validate the contact model.

Acknowledgments We gratefully acknowledge partial support of this work by Mr. Edward B. Fanslau, Hanya-san of the NHK International Corp. L. Li would like to thank the China Scholarship Council (CSC) and Prof. G. Zhang from Harbin Institute of Technology for supporting his PhD study at UCSD.

Open Access This article is distributed under the terms of the Creative Commons Attribution Noncommercial License which permits any noncommercial use, distribution, and reproduction in any medium, provided the original author(s) and source are credited.

References

1. Johnson, K.L.: *Contact Mechanics*. Cambridge University Press, Cambridge (1985)
2. Greenwood, J.A., Williamson, J.B.P.: Contact of nominally flat surfaces. *Proc. R. Soc. Lond. A* **295**, 300–319 (1966)
3. Greenwood, J.A., Tripp, J.H.: The elastic contact of rough spheres. *J. Appl. Mech. Trans. ASME* **34**, 153–159 (1967)
4. Kagami, J., Yamada, K., Hatazawa, T.: Contact between a sphere and rough plates. *Wear* **87**, 93–105 (1983)
5. Greenwood, J.A., Johnson, K.L., Matsubaru, E.: A surface roughness parameter in hertz contact. *Wear* **100**, 47–57 (1984)
6. Bahrami, M., Yovanovich, M.M., Culham, J.R.: A compact model for spherical rough contacts. *J. Tribol. Trans. ASME* **127**, 884–889 (2005)
7. Wang, F.S., Block, J.M., Chen, W.W., Martini, A., Zhou, K., Keer, L.M., Wang, Q.J.: A multilevel model for elastic-plastic contact between a sphere and a flat rough surface. *J. Tribol. Trans. ASME* **131**, 021409 (2009)
8. Jamari, J., Schipper, D.J.: Displacement due to contact between a rough surface and a smooth ball. *J. Tribol. Trans. ASME* **262**, 138–145 (2007)
9. Cohen, D., Kligerman, Y., Etsion, I.: The effect of surface roughness on static friction and junction growth of an elastic-plastic spherical contact. *J. Tribol. Trans. ASME* **131**, 021404 (2009)
10. Li, L., Etsion, I., Talke, F.E.: Contact area and static friction of rough surfaces with high plasticity index. *J. Tribol. Trans. ASME* **262**, 138–145 (2010)
11. Brizmer, V., Kligerman, Y., Etsion, I.: The effect of contact conditions and material properties on the elasticity terminus of a spherical contact. *Int. J. Solids Struct.* **43**, 5736–5749 (2006)
12. Kogut, L., Etsion, I.: A finite element based elastic-plastic model for the contact of rough surfaces. *Tribol. Trans.* **46**, 383–390 (2003)
13. Kogut, L., Etsion, I.: Elastic-plastic contact analysis of a sphere and a rigid flat. *J. Appl. Mech. Trans. ASME* **69**, 657–662 (2002)
14. Yeo, C., Katta, R., Polycarpou, A.: Improved elastic contact model accounting for asperity and bulk substrate deformation. *Tribol. Lett.* **35**, 191–203 (2009)
15. Ovcharenko, A., Halperin, G., Etsion, I.: Experimental study of adhesive static friction in a spherical elastic-plastic contact. *J. Tribol. Trans. ASME* **130**, 021401 (2008)
16. Ovcharenko, A., Halperin, G., Etsion, I.: In situ and real time optical investigation of junction growth in spherical elastic-plastic contact. *Wear* **264**, 1043–1050 (2008)
17. Jeng, Y.-R., Peng, S.-R.: Investigation into the lateral junction growth of single asperity contact using static atomistic simulations. *Appl. Phys. Lett.* **94**, 163103 (2009)
18. Nix, W.D., Gao, H.: Indentation size effects in crystalline materials: a law for strain gradient plasticity. *J. Mech. Phys. Solids* **46**, 411–425 (1998)